

Alma Mater Studiorum Università di Bologna
Archivio istituzionale della ricerca

Sulfide affects the mitochondrial respiration, the Ca^{2+} -activated F1FO-ATPase activity and the permeability transition pore but does not change the Mg^{2+} -activated F1FO-ATPase activity in swine heart mitochondria

This is the final peer-reviewed author's accepted manuscript (postprint) of the following publication:

Published Version:

Nesci, S., Algieri, C., Trombetti, F., Ventrella, V., Fabbri, M., Pagliarani, A. (2021). Sulfide affects the mitochondrial respiration, the Ca^{2+} -activated F1FO-ATPase activity and the permeability transition pore but does not change the Mg^{2+} -activated F1FO-ATPase activity in swine heart mitochondria. PHARMACOLOGICAL RESEARCH, 166, 105495-105504 [10.1016/j.phrs.2021.105495].

Availability:

This version is available at: <https://hdl.handle.net/11585/821253> since: 2021-05-31

Published:

DOI: <http://doi.org/10.1016/j.phrs.2021.105495>

Terms of use:

Some rights reserved. The terms and conditions for the reuse of this version of the manuscript are specified in the publishing policy. For all terms of use and more information see the publisher's website.

This item was downloaded from IRIS Università di Bologna (<https://cris.unibo.it/>).
When citing, please refer to the published version.

(Article begins on next page)

This is the final peer-reviewed accepted manuscript of:

Sulfide affects the mitochondrial respiration, the Ca^{2+} -activated F_1F_0 -ATPase activity and the permeability transition pore but does not change the Mg^{2+} -activated F_1F_0 -ATPase activity in swine heart mitochondria.

Nesci S, Algieri C, Trombetti F, Ventrella V, Fabbri M, Pagliarani A. Pharmacol Res. 2021;166:105495.

The final published version is available online at: **<https://doi-org.ezproxy.unibo.it/10.1016/j.phrs.2021.105495>**

Rights / License:

The terms and conditions for the reuse of this version of the manuscript are specified in the publishing policy. For all terms of use and more information see the publisher's website.

This item was downloaded from IRIS Università di Bologna (<https://cris.unibo.it/>)

When citing, please refer to the published version.

Sulfide affects the mitochondrial respiration, the Ca^{2+} -activated F_1F_0 -ATPase activity and the permeability transition pore but does not change the Mg^{2+} -activated F_1F_0 -ATPase activity in swine heart mitochondria

Salvatore Nesci*, Cristina Algieri, Fabiana Trombetti, Vittoria Ventrella, Micaela Fabbri, Alessandra Pagliarani

Department of Veterinary Medical Sciences (DIMEVET), University of Bologna, via Tolara di Sopra, 50, 40064 Ozzano Emilia (Bologna), Italy.

*Corresponding author: salvatore.nesci@unibo.it. Department of Veterinary Medical Sciences (DIMEVET), University of Bologna, via Tolara di Sopra, 50, 40064 Ozzano Emilia (Bologna), Italy.

Keywords: H_2S ; mitochondria; mitochondrial respiration; F_1F_0 -ATPase; permeability transition pore; cofactors.

Abstract

In mammalian cells enzymatic and non-enzymatic pathways produce H_2S , a gaseous transmitter which recently emerged as promising therapeutic agent and modulator of mitochondrial bioenergetics. To explore this topic, the H_2S donor NaHS, at micromolar concentrations, was tested on swine heart mitochondria. NaHS did not affect the F_1F_0 -ATPase activated by the natural cofactor Mg^{2+} , but, when Mg^{2+} was replaced by Ca^{2+} , a slight 15% enzyme inhibition at 100 μM NaHS was shown. Conversely, both the NADH-O_2 and succinate- O_2 oxidoreductase activities were totally inhibited by 200 μM NaHS with IC_{50} values of 61.6 ± 4.1 and 16.5 ± 4.6 μM NaHS, respectively. Since the mitochondrial respiration was equally inhibited by NaHS at both first or second respiratory substrates sites, the H_2S generation may prevent the electron transfer from complexes I and II to downhill respiratory chain complexes, probably because H_2S competes with O_2 in complex IV, thus reducing membrane potential as a consequence of the cytochrome c oxidase activity inhibition. The Complex IV blockage by H_2S was consistent with the linear concentration-dependent NADH-O_2 oxidoreductase inhibition and exponential succinate- O_2 oxidoreductase inhibition by NaHS, whereas the coupling between substrate oxidation and phosphorylation was unaffected by NaHS. Even if H_2S is known to cause sulfhydration of cysteine residues, thiol oxidizing (GSSG) or reducing (DTE) agents, did not affect the F_1F_0 -ATPase activities and mitochondrial respiration, thus ruling out any involvement of post-translational modifications of thiols. The permeability transition pore, the lethal channel which forms when the F_1F_0 -ATPase is stimulated by Ca^{2+} , did not open in the presence of NaHS, which shows a similar effect to ruthenium red, thus suggesting a putative Ca^{2+} transport cycle inhibition.

1. Introduction

Mitochondrial bioenergetics relies on substrate oxidation during mitochondrial respiration to generate a transmembrane electrochemical gradient of H^+ ($\Delta\mu_{H^+}$) that drives ADP phosphorylation to produce ATP [1]. The oxidative phosphorylation (OXPHOS) system in the inner mitochondrial membrane (IMM) basically consists of respiratory chain complexes that transfer reducing equivalents from NADH or $FADH_2$ ultimately to oxygen. According to the chemiosmotic hypothesis, the downhill electron flow through these enzyme complexes allows H^+ pumping by complex (C) I, III and IV in the intermembrane space, while the CII cannot pump H^+ . Finally, the OXPHOS coupling between the transmembrane H^+ gradient formation and ATP synthesis is provided by the ATP synthase or F_1F_0 -ATPase, which exploits the $\Delta\mu_{H^+}$ to synthesize ATP [2]. The respiratory complexes (RC) transfer electrons from NADH to O_2 by CI, CIII and finally CIV. $FADH_2$, which receives electrons from succinate, follows a shorter route, namely CII, CIII and CIV [3]. RC can function separately or assemble in supercomplexes of defined stoichiometry [4], without involving CII. Recent studies on mammalian heart mitochondria showed that the individual complexes form the so-called respirasome [5,6] whose stoichiometry varies from the respiratory supercomplex ($CI_1+CIII_2+CIV_1$) to the megacomplex ($CI_2+CIII_2+CIV_2$) [7]. In addition, the CIII dimer may assemble with CIV ($CIII_2+CIV_1$) or CI (CI_1+CIII_2) [8]. The (CI_1+CIII_2) assembly may decrease the production of reactive oxygen species [9] and favour respirasome formation [10]. Moreover, the dimerization of CV (the F_1F_0 -ATPase) intervenes in membrane bending and in the formation of the *cristae* [11,12]. The main role of the F_1F_0 -ATPase in mitochondria is to produce ATP in F_1 [13], driven by H^+ flow through the membrane-embedded F_0 domain [14]. The two functionally and structurally coupled domains allow the $\Delta\mu_{H^+}$ transduction into ATP formation and *vice versa* [15,16]. The ubiquitous F_1F_0 -ATPase occurs in bacteria, chloroplasts and mitochondria [17]. In mitochondria supernumerary subunits (SNS) [18], would confer to the F_1F_0 -ATPase dimer the capability of arranging in rows and of opening the permeability transition pore (PTP) [19]. Accordingly, the F_0 domain of the F_1F_0 -ATPase, and particularly its core or c-ring, contains a lipid plug whose expulsion forms the hole, namely the main conductance channel known as PTP [18]. This molecular event is triggered by conformational changes driven by the replacement of the natural cofactor Mg^{2+} bound to the F_1 domain by Ca^{2+} , when Ca^{2+} concentration increases in the matrix under patho(physio)logical conditions [20]. On these bases, most likely the Ca^{2+} -activated F_1F_0 -ATPase inhibition can counteract the PTP formation and prevent or delay cell death [21]. Since the mPTP dysregulation is involved in the pathogenesis of various diseases [22], PTP rulers, which are an emerging topic to be investigated, may play the role of drugs.

Hydrogen sulphide (H_2S) is an endogenous gaseous transmitter, which shares some of the signalling pathways with other endogenously produced gases [23], to mediate vascular remodelling and angiogenesis. By involving cyclic nucleotides as second messengers, the cardiovascular system and inflammation mechanisms are modulated by H_2S [24]. Due to its lipophilicity and low molecular weight, H_2S can easily cross biomembranes and chemically modify cell proteins by inducing post-translational modifications which affect their structure and function. The sulfhydration by H_2S is a post-translational modifications of cysteine residues: the cysteine thiol (-SH) binds sulfur to yield hydropersulfide (-SSH). The F_1F_0 -ATPase can undergo persulfidation to modulate cell bioenergetics [25,26]. As many exogenous and endogenous compounds, H_2S is a Janus molecule that can show both beneficial and toxic effects: beneficial effects predominate at micro and nanomolar concentrations while at high concentrations, H_2S is a known mitochondrial poison [27]. In the present work, the effects of the widely used H_2S donor NaHS on the whole mitochondrial energy-converting enzymes are explored. The results can contribute to highlight the multiple and still partially unknown action mechanisms of this inorganic modulator in mammalian mitochondria and help to understand the molecular basis of its therapeutic potential.

2. Experimental Procedures

2.1. Chemicals

NaHS, oligomycin (a mixture of oligomycins A, B and C), antimycin A, Ruthenium Red, Fura-FF, and JC-10 were purchased from Vinci-Biochem (Vinci, Italy). Cytochrome *c*, rotenone, NADH, succinate, Na₂ATP, 1,4-dithioerythritol (DTE), dithiotreitol (DTT) and oxidized L-glutathione (GSSG) were obtained from Sigma-Aldrich (Milan, Italy). Quartz double distilled water was used for all reagent solutions.

2.2. Preparation of mitochondrial fractions

Swine hearts (*Sus scrofa domesticus*) were collected at a local abattoir and transported to the lab within 2 h in ice buckets at 0–4°C. After removal of fat and blood clots as much as possible, approximately 30–40 g of heart tissue were rinsed in ice-cold washing Tris-HCl buffer (medium A) consisting of 0.25 M sucrose, 10 mM Tris(hydroxymethyl)-aminomethane (Tris), pH 7.4 and finely chopped into fine pieces with scissors. Each preparation was made from one heart. Once rinsed, tissues were gently dried on blotting paper and weighted. Then tissues were homogenized in medium B consisting of 0.25 M sucrose, 10 mM Tris, 1 mM EDTA (free acid), 0.5 mg/mL BSA fatty acid free, pH 7.4 with HCl at a ratio of 10 mL medium B per 1 g of fresh tissue. After a preliminary gentle break up by Ultraturrax T25, the tissue was carefully homogenized by a motor-driven teflon pestle homogenizer (Braun Melsungen Type 853202) at 650 rpm with 3 up-and-down strokes. The mitochondrial fraction was then obtained by stepwise centrifugation (Sorvall RC2-B, rotor SS34). Briefly, the homogenate was centrifuged at 1,000 \times g for 5 min, thus yielding a supernatant and a pellet. The pellet was re-homogenized under the same conditions of the first homogenization and re-centrifuged at 1,000 \times g for 5 min. The gathered supernatants from these two centrifugations, filtered through four cotton gauze layers, were centrifuged at 10,500 \times g for 10 min to yield the raw mitochondrial pellet. The raw pellet was resuspended in medium A and further centrifuged at 10,500 \times g for 10 min to obtain the final mitochondrial pellet. The latter was resuspended by gentle stirring using a Teflon Potter Elvehjem homogenizer in a small volume of medium A, thus obtaining a protein concentration of 30 mg/mL [28]. All steps were carried out at 0–4°C. The protein concentration was determined according to the colorimetric method of Bradford [29] by Bio-Rad Protein Assay kit II with BSA as standard. The mitochondrial preparations were then stored in liquid nitrogen until the evaluation of F-ATPase activities.

2.3. Mitochondrial F-ATPase activity assays

Thawed mitochondrial preparations were immediately used for F-ATPase activity assays. The capability of ATP hydrolysis was assayed in a reaction medium (1 mL) containing 0.15 mg mitochondrial protein and 75 mM ethanolamine-HCl buffer pH 9.0, 6.0 mM Na₂ATP and 2.0 mM MgCl₂ for the Mg²⁺-activated F₁F₀-ATPase assay, and 75 mM ethanolamine-HCl buffer pH 8.8, 3.0 mM Na₂ATP and 2.0 mM CaCl₂ for the Ca²⁺-activated F₁F₀-ATPase assay. These assay conditions were previously proven to elicit the maximal enzyme activities either stimulated by Mg²⁺ or by Ca²⁺ in swine heart mitochondria [30]. After 5 min preincubation at 37°C, the reaction, carried out at the same temperature, was started by the addition of the substrate Na₂ATP and stopped after 5 min by the addition of 1 mL of ice-cold 15% (w/w) trichloroacetic acid aqueous solution. Once the reaction was stopped, vials were centrifuged for 15 min at 3,500 rpm (Eppendorf Centrifuge 5202). In the supernatant, the concentration of inorganic phosphate (Pi) hydrolyzed by known amounts of mitochondrial protein, which is an indirect measure of F-ATPase activity, was spectrophotometrically evaluated [31]. To this aim, 1 μ L from a mother solution of 3 mg/mL oligomycin in dimethylsulfoxide was directly added to the reaction mixture before starting the reaction. The total ATPase activity was calculated

by detecting the Pi in control tubes run in parallel and containing 1 μ L dimethylsulfoxide per mL reaction system. In each experimental set, control tubes were alternated to the condition to be tested. The employed concentration of oligomycin, specific inhibitor of F-ATPases which selectively blocks the F_0 subunit ensured maximal enzyme activity inhibition and was currently used in F-ATPase assays [20]. The F_1F_0 -ATPase activity was routinely measured by subtracting, from the Pi hydrolyzed by total ATPase activity, the Pi hydrolyzed in the presence of oligomycin [28]. In all experiments the F-ATPase activity was expressed as μ mol Pi·mg protein⁻¹·min⁻¹. The effects of the NaHS were tested by adding 10 μ L aliquots of standard NaHS solutions in DMSO to the reaction mixture immediately prior to the addition of the mitochondrial suspensions. The reaction system containing NaHS and mitochondria were preincubated at 37°C for 5 min before starting the ATPase reaction by ATP addition. To this aim, aliquots of DMSO solutions of appropriate NaHS concentrations, obtained by dilution from the mother 50 mM NaHS solution in DMSO, were added to the reaction mixture to obtain the final NaHS concentrations in the range 0.1–100 μ M NaHS in the reaction system. Preliminary assays showed that, under the conditions adopted, DMSO had no effect on the ATPase activities under study. The effects of 50 μ M DTE and 1 mM GSSG were tested by adding 10 μ L aliquots of thiol reagent solutions in H₂O to the reaction mixture at the time of the preincubation before starting the ATPase reaction.

2.4. Mitochondrial respiration assays

Immediately after thawing, the mitochondrial fractions were used to evaluate the mitochondrial respiration. The experimental conditions adopted ruled out any potential concomitant effect of changes in the transmembrane electrochemical gradient of H⁺. To detect mitochondrial respiratory activities, the oxygen consumption rates were polarographically evaluated by Clark-type electrode using a thermostated Oxytherm System (Hansatech Instruments) equipped with a 1 mL polarographic chamber. The reaction mixture (120 mM KCl, 10 mM Tris-HCl buffer pH 7.2), maintained under Peltier thermostatisation at 37°C and continuous stirring, contained 0.25 mg mitochondrial protein [32].

To evaluate the NADH-O₂ oxidoreductase activity, the mitochondrial oxidation was run under saturating substrate conditions (75 μ M NADH) after 2 min of stabilization of the oxygen signal. Preliminary tests assessed that under these conditions O₂ consumption was suppressed by 2.5 μ M rotenone, known inhibitor of CI. [3] The succinate-O₂ oxidoreductase activity by CII was evaluated by detecting the succinate oxidation in the presence of 2.5 μ M rotenone. The reaction was started by the addition of 10 mM succinate after 2 min of stabilization of oxygen signal. Also in this case preliminary tests assessed that, under the conditions applied, succinate oxidation was suppressed by 1 μ g/mL antimycin A, selective inhibitor of CIII [3].

To evaluate the effects of NaHS, the reaction was started by the addition of the mitochondrial suspensions to the polarographic chamber at 37°C. Aliquots from mother solutions in DMSO and DTE in H₂O, prepared immediately before the experiments, were added to the polarographic chamber at the reaction start, sequentially or in reverse order when required, to obtain the final NaHS and DTE concentrations to be tested. The mitochondrial respiratory rate was automatically evaluated by O₂view software and expressed as nmoles O₂·mg protein⁻¹·min⁻¹. Polarographic assays were run at least in triplicate on mitochondrial preparations obtained from different animals.

2.5. Evaluation of oxidative phosphorylation

Immediately after the preparation of the mitochondrial fraction, the mitochondrial respiratory activity was polarographically evaluated by Clark-type electrode using a thermostated Oxytherm System (Hansatech

Instruments) in terms of oxygen consumption at 37°C in a 1 mL polarographic chamber. The reaction mixture, maintained under thermostatisation and continuous stirring, contained 0.25 mg/mL mitochondrial suspension, 40 mM KCl, 0.2 mg/mL fatty acid-free BSA, 75 mM sucrose, 0.5 mM EDTA, 30 mM Tris-HCl, pH 7.4, 5 mM KH_2PO_4 plus 3 mM MgCl_2 . In detail, the rate of oxygen consumption was evaluated in the presence of specific substrates, namely glutamate/malate (1:1), for CI, succinate for CII, and in the presence of 1 µg/mL rotenone, to inhibit CI, and 1 µM antimycin A to inhibit CIII. Glutamate/malate oxidation was taken as a measure of the activity of NADH: ubiquinone oxidoreductase; succinate oxidation mirrored the multi-component succinoxidase pathway, which accounts for the electron flux in the respiratory chain through CII. To evaluate mitochondrial integrity, since intact mitochondrial membranes are not permeable to NADH, during the polarographic assay in the presence of glutamate/malate as substrate, 75 µM NADH were added to the reaction mixture. Coupling of respiratory activity to phosphorylation was evaluated by adding 150 nmol ADP to state 2 respiring mitochondria [33,34]. The NaHS mother solution (50 mM NaHS) was prepared immediately before the experiments by dissolving NaHS in DMSO. This solution was used to obtain by further dilutions NaHS solutions of adequate concentrations, in order to minimize DMSO input in the reaction system. Preliminary experiments showed that addition of small DMSO aliquots (up to 5 µL) to the reaction system (1 mL) did not affect the respiratory rates. Micromolar concentrations of NaHS in the reaction system were tested. Respiratory activities were evaluated as nmoles $\text{O}_2 \cdot \text{mg protein}^{-1} \cdot \text{min}^{-1}$. In routine experimental protocol, reagents were injected by a syringe into the polarographic cell containing the mitochondrial protein suspensions in the presence and in the absence of NaHS in the following order: inhibitors of the previous respiratory chain steps, when required, substrate(s), ADP, inhibitor (rotenone for glutamate/malate stimulated respiration and antimycin A for succinate-stimulated respiration). State 3 and 4 respiratory activities, the respiratory control ratio (RCR), namely the ratio between State 3 and 4 activities, were determined as defined by Chance and Williams [33–35]. The rate of oxygen consumption was assessed in the presence of the specific substrates glutamate/malate for CI, succinate for CII. Polarographic assays were run at least in triplicate on three mitochondrial preparations from different animals.

2.6. Evaluation of cytochrome c oxidase activity

The polarographic assay of the cytochrome c-oxidase activity, even if currently employed, may cause interference due to the possible concomitant oxidation of the substrate ascorbate+*N,N,N',N'*-Tetramethyl-p-phenylenediamine dihydrochloride (TMPD) in the presence of NaHS, known to exhibit reducing properties [36,37]. Therefore, the evaluation of the cytochrome c oxidase activity was carried out according to the colorimetric method detailed below.

The colorimetric assay, based on the detection of the decrease in absorbance at 550 nm of ferrocytochrome c, caused by its oxidation by the cytochrome c oxidase, was carried out on the basis of Sigma cytochrome c oxidase assay kit (Product Code: CYTOC-OX1) and adequately adapted. In order to obtain a reduced cytochrome c (cyt c) solution, the reducing agent dithiothreitol (DTT) was added to a 0.22 mM cyt c aqueous solution to yield a final concentration of 0.5 mM DTT, gently mixed and let to react for 15 min at room temperature. The cyt c reduction state was evaluated by 1:20 diluting the reduced cyt c solution with the assay buffer solution (10 mM Tris/HCl, pH 7.0, 120 mM KCl) and by recording the absorbance (A) at 550 and 565 nm by Perkin–Elmer lambda 45 spectrophotometer (Perkin–Elmer, Massachusetts, USA); a A_{550}/A_{565} ratio in the range 10–20 was taken as indicative of an adequately reduced cyt c. Both solutions of reduced cyt c and NaHS were prepared just before the enzyme activity analysis. Preliminary experiments showed that up to 10 µL DMSO added to the reaction mixture (2 mL) did not affect the enzyme activity. To evaluate the cytochrome c oxidase activity, 0.4 mg mitochondrial protein were added to the assay buffer to a final volume

of 2 mL in a 25°C thermostated cuvette under continuous stirring. The reaction was started by adding aliquots of the reduced cyt c solution to yield a 10 µM cyt c in the reaction mixture. The initial rate of cyt c oxidation, measured by following the A₅₅₀ nm decrease up to 45'' from cyt c addition, was evaluated by Perkin–Elmer UV KinLab Software [38]. Increasing NaHS concentrations, directly added to the reaction mixture before starting the enzymatic reaction, were tested. Control tests, in which the reaction was carried out in a NaHS free medium under the same assay conditions were alternated to assays in NaHS containing samples. Each experiment was run in triplicate. The cytochrome c oxidase activity was expressed as oxidized cyt c units (U)/mL, where 1 U corresponds to 1 µmol cyt c oxidized per min.

2.7. Evaluation of PTP and membrane potential

Immediately after the preparation of swine heart mitochondrial fractions, fresh mitochondrial suspensions (1mg/mL) were energized in the assay buffer (130 mM KCl, 1 mM KH₂PO₄, 20 mM HEPES, pH 7.2 with TRIS), incubated at 25°C with 1 µg/mL rotenone and 5 mM succinate as respiratory substrate. To evaluate NaHS effect, selected NaHS concentrations were added to the mitochondrial suspensions before PTP evaluation. PTP opening was induced by the addition of low concentrations of Ca²⁺ (10 µM) as CaCl₂ aqueous solution at fixed time intervals (1 min). The calcium retention capacity (CRC), whose lowering indicates mPTP opening, was spectrofluorophotometrically evaluated in the presence of 0.8 µM Fura-FF. The probe has different spectral properties in the absence and in the presence of Ca²⁺, namely it displays excitation/emission spectra of 365/514 nm in the absence of Ca²⁺ (Fura-FF low Ca²⁺) and shifts to 339/507 nm in the presence of high Ca²⁺ concentrations (Fura-FF high Ca²⁺). PTP opening, was evaluated by the increase in the fluorescence intensity ratio (Fura-FF high Ca²⁺)/(Fura-FF low Ca²⁺), which indicates a decrease in CRC. The membrane potential (Δφ) was evaluated in presence of 0.5 µM JC-10. In polarized mitochondrial membranes, this probe selectively generates an orange JC-10 aggregate (excitation/emission spectra of 540/590 nm). The JC-10 monomers, generated when Δφ decreases, cause a green shift (excitation/emission spectra of 490/525 nm). Accordingly, the membrane depolarization (decrease in Δφ) ascribed to PTP formation was detected by the increase in the fluorescence intensity ratio which corresponds to an increased JC-10 aggregate/JC-10 monomers ratio. [20,39]. All measurements were processed by LabSolutions RF software.

2.8. Calculations and statistics

The data represent the mean ± SD (shown as vertical bars in the figures) of the number of experiments reported in the figure captions. In each experimental set, the analyses were carried out on different pools of animals. Statistical analyses were performed by SIGMASTAT software. The analysis of variance followed by Students–Newman–Keuls' test when F values indicated significance (*P*≤0.05) was applied. Percentage data were *arcsin*-transformed before statistical analyses to ensure normality.

3. Results

3.1. NaHS effects on the F₁F₀-ATPase and thiol redox state

In order to evaluate the effect of NaHS on the F₁F₀-ATPase activated by Mg²⁺ or by Ca²⁺, the enzyme activities were evaluated in the range of 0.1 – 100 µM NaHS (Fig. 1). The Mg²⁺-dependent F₁F₀-ATPase was refractory to all NaHS concentrations tested (Fig. 1A). In contrast, the Ca²⁺-dependent F₁F₀-ATPase was inhibited about 15% by 100 µM NaHS (Fig. 1B). The same effect on the Mg²⁺- and Ca²⁺-dependent F₁F₀-ATPases was observed

with freshly extracted mitochondria, which were not stored in liquid nitrogen (Fig. S1). Since NaHS was reported to form persulfide (–SSH) groups by modifying cysteine thiols, this possibility was verified by testing the NaHS effect in presence of thiol reducing/oxidizing agents, *i.e.* DTE and GSSG, on the F_1F_0 -ATPase activity either activated by Ca^{2+} or by Mg^{2+} (Fig. 2). In the presence of 50 μ M DTE or 1 mM GSSG the Mg^{2+} -dependent F_1F_0 -ATPase (Fig. 2A,C) was unaffected. Similarly, the Ca^{2+} -dependent F_1F_0 -ATPase in presence of 50 μ M DTE and 1 mM GSSG (Fig. 2B,D) showed a similar enzyme activity to the control (without DTE and NaHS). The significant Ca^{2+} -dependent F_1F_0 -ATPase inhibition by 100 μ M NaHS, even if around 15%, was reduced by DTE but remained detectable with respect to the control (Fig. 2B). Conversely, 1 mM GSSG did not significantly change the Ca^{2+} -dependent F_1F_0 -ATPase activity either in the presence or in the absence of 100 μ M NaHS (Fig. 2D).

3.2. NaHS effects on mitochondrial respiratory complexes

The effects of NaHS on mitochondrial respiration were evaluated in NADH- and succinate-energized mitochondria (Fig. 3). The effects of micromolar NaHS concentrations up to 100 μ M, were tested by detecting the oxygen consumption in uncoupled (freeze-thawed) mitochondria in the presence of either NADH or succinate as substrates, which stimulate the activity of CI (NADH) and CII (succinate). The substrate-depending inhibition potency of NaHS, estimated as IC_{50} values, was calculated as 15.4 ± 3.7 μ M for the NADH- O_2 oxidoreductase activity (Fig. 3A) and 16.3 ± 6.2 μ M for the Succinate- O_2 oxidoreductase activity (Fig. 3B). The Succinate- O_2 oxidoreductase activity was also strongly reduced by a sigmoidal concentration-response profile. In order to understand whether NaHS inhibition on mitochondrial respiration mirrors a putative –SSH post-translational modification of enzyme cysteines, known as susceptible to oxidation, the thiol-reagent DTE, which maintains thiols reduced and prevents their oxidation, was tested (Fig. 4). However DTE had no significant effect on the NADH- O_2 and Succinate- O_2 oxidoreductase activities (Fig. 4A,C) and did not remove the inhibition by NaHS. To rule out a direct reaction between DTE and NaHS, the NADH- O_2 and succinate- O_2 oxidoreductase activities were evaluated by adding DTE before and after NaHS. In all cases the NaHS-driven inhibition on mitochondrial respiration was not reverted by DTE (Fig. 4B,D).

Since the respiration inhibition by NaHS was downstream maintained from CI to CII, the cytochrome *c* oxidase activity, which mirrors the activity of CIV was evaluated. Also in this case, NaHS concentration-dependently inhibited cytochrome *c* oxidation (Fig. 5), showing an IC_{50} value of 65.8 ± 6.6 μ M NaHS, namely similar to that of the NADH- O_2 oxidoreductase. In order to understand the relationship between substrate oxidation by mitochondrial complexes and NaHS inhibition on the individual complexes, threshold plots were built. To this aim, the residual activity of NADH- O_2 (Fig. 6A) and succinate- O_2 oxidoreductases (Fig. 6B) detected at fixed NaHS concentrations were plotted as a function of the corresponding cytochrome *c* oxidase inhibition percentage (Fig. 6). These plots highlighted that the cytochrome *c* oxidase inhibition by NaHS was exponentially linked to the inhibition of the NADH- O_2 oxidoreductase activity (Fig. 6A) or to the succinate- O_2 oxidoreductase inhibition (Fig. 6B).

The results obtained when 30 μ M NaHS was added to state 3 respiring (ADP-stimulated) mitochondria showed a prompt decrease in oxygen consumption, both in the presence of NAD-dependent substrates (Fig. 7A) and in the presence of succinate (Fig. 7B). A significantly lower respiration occurred in state 4 respiratory activity, which mirrors the slowdown in oxygen consumption when added ATP is consumed, being phosphorylated to ATP. However, the coupling between substrate oxidation (glutamate/malate or succinate) and ADP phosphorylation, evaluated as State 3/State 4 ratio, was unaffected by NaHS (Fig. 7).

3.3. PTP opening and membrane potential sensitivity to the NaHS

The IMM integrity implies that mitochondria retain calcium and do not form the PTP. Ca^{2+} concentration increase in mitochondria stimulates PTP formation and opening. On these bases, the CRC was evaluated by adding $10\ \mu\text{M}\ \text{Ca}^{2+}$ at subsequent steps of 1 min to succinate-energized freshly-prepared mitochondrial suspensions. According to the method applied, a detectable increase in fluorescence intensity, detected as Fura-FF ratio $[(\text{Fura-FF high Ca}^{2+})/(\text{Fura-FF low Ca}^{2+})]$, was shown when a threshold matrix Ca^{2+} concentration load was attained as a result of PTP opening. In control mitochondria the CRC decrease was revealed after 200'' upon a two-train Ca^{2+} pulses. In the presence of the polycationic dye ruthenium red (RR), the PTP is known to be desensitized, due to the failed Ca^{2+} accumulation in the matrix caused by the selective RR inhibition of the mitochondrial calcium uniporter [40]. The two NaHS concentrations tested (50 and $100\ \mu\text{M}$), selected on the basis of IC_{50} values obtained on mitochondrial respiration and on the Ca^{2+} -activated F_1F_0 -ATPase, did not elicit any sudden increase in fluorescence intensity due to Ca^{2+} release. Indeed, the rate of Ca^{2+} uptake could be altered, as the time required to regain the basal $[\text{Ca}^{2+}]$ after each Ca^{2+} pulse was different from that of the control and a gradual baseline increase was shown. Quite unexpectedly, NaHS and RR resulted in the similar trend, thus suggesting a common target, namely the inhibition of the mitochondrial calcium uniporter (Fig. 8A).

In order to improve clarity on the NaHS effects on PTP formation, $\Delta\phi$, namely the transmembrane potential, which is abruptly dissipated by PTP opening, was evaluated. As shown in Figure 6A, in control mitochondria, the CRC decrease at the second Ca^{2+} pulse corresponded to the $\Delta\phi$ collapse, shown by the JC-10 ratio increase (Fig. 8B). To verify that the PTP formation depolarizes the mitochondria, $0.1\ \mu\text{M}$ FCCP were added after the JC-10 ratio increase produced by Ca^{2+} shots, but no increase in mitochondrial depolarization was recorded (data not shown). NaHS both at 50 and $100\ \mu\text{M}$ only caused a gradual $\Delta\phi$ decrease, which most likely could be related to the inhibition of mitochondrial respiration and its related H^+ pumping activities, rather than to PTP opening.

4. Discussion

The effects of H_2S on mitochondrial bioenergetics has been extensively investigated and reviewed (see reviews and references therein [27,41,42]). The present work may represent an attempt to deepen the effects of NaHS concentrations, assumed to generate H_2S , on the various components of the bioenergetic machinery in mitochondria isolated from swine heart, an excellent model to investigate drug effects in translational medicine, especially in the perspective of counteracting cardiovascular diseases. Of the three sulfide forms, which coexist in aqueous solution in an interconverting pH dependent-equilibrium, namely HS^- , S^{2-} and H_2S , at physiological pH, H_2S is the most likely candidate to directly affect mitochondrial proteins, since it can easily cross biomembranes due to its lipophilicity and lack of electric charge. The F_1F_0 -ATPase was reported to be sulfhydrated or S-sulfurated, by using the correct term [43], by the H_2S donor NaHS. The H_2S target was identified on α subunit at Cys244 and Cys294 in HepG2 and HEK293 cell lysates incubated with $100\ \mu\text{M}$ NaHS for 30 min at 37°C . Moreover, the F_1F_0 -ATPase activity showed a bell-shaped concentration-response curve in the range of $0.01 - 100\ \mu\text{M}$ NaHS [25]. Post-translational modifications on the F_1F_0 -ATPase are well known to modulate the enzyme function [26]. However, in swine heart mitochondria NaHS, at the same concentrations proven to be effective on the F_1F_0 -ATPase in HepG2 and HEK293 cells, has not effect on the ATP hydrolytic activity of the Mg^{2+} -activated F_1F_0 -ATPase. Conversely, the Ca^{2+} -activated F_1F_0 -ATPase, whose enzymatic function is linked to PTP opening [20,39], is slightly inhibited by $100\ \mu\text{M}$ NaHS (Fig. 1). Most likely metabolic and signaling pathways might explain the F_1F_0 -ATPase responsiveness to H_2S in intact cells. Moreover, in swine heart mitochondria the weak even if significant Ca^{2+} -activated F_1F_0 -ATPase inhibition by

100 μM NaHS is not due to any post-translational modification of cysteine thiols. Accordingly, the addition of thiol reagents, namely oxidizing (GSSG) and reducing (DTE) low molecular weight thiols maintains the Mg^{2+} -activated F_1F_0 -ATPase refractoriness to NaHS and the slight inhibition of the Ca^{2+} -activated F_1F_0 -ATPase activity (Fig. 2), thus ruling out the possibility of any direct sulfide reaction with F_1F_0 -ATPase thiols.

On considering the F_1F_0 -ATPase insensitivity to NaHS, sulfide effects were investigated on respiratory complexes. Freeze-thawed uncoupled mitochondria, insensitive to the uncoupler FCCP (data not shown) were used to evaluate mitochondrial respiration by adding CI (NADH) and CII (succinate) respiratory substrates. Even if both CI and CII were inhibited by NaHS, the inhibition extent is about three-fold higher on CII, as shown by the decreased succinate- O_2 oxidoreductase activity (Fig. 3). Since in both cases the inhibition is not reversed by DTE, which can reduce the persulfide groups (Fig. 4), post-translational modifications of protein thiols cannot be responsible for the inhibition of the enzyme activities. The electron transfer from both substrates (NADH and succinate) to O_2 in the respiratory chain is blocked downstream. Accordingly, the well known H_2S inhibition of CIV [44] is confirmed by present data on the cytochrome c oxidase inhibition (Fig. 5). Moreover, at low concentrations H_2S is known as the first inorganic electron donor to the mitochondrial electron transport chain through sulfide:quinone oxidoreductase (SQR) and CII, thereby stimulating mitochondrial respiration [45,46]. For this reason, the more pronounced H_2S inhibition on the succinate- O_2 oxidoreductase, which shows an exponential enzyme activity decrease at increasing NaHS concentrations, than on the NADH- O_2 oxidoreductase may be due to a competitive coenzyme Q_{10} reduction between SQR and succinate dehydrogenase activities. As CII do not participate in the respirasome assembly, whose supramolecular organization ensures a homogeneous distribution and a functionally relevant interaction between complexes in the membrane [10,47], H_2S and succinate may mutually exclude as electron donors to the respiratory chain. This mechanism may add to CIV inhibition in slowing down the respiratory chain (Fig. 6). The insensitivity of the Mg^{2+} -activated F_1F_0 -ATPase to NaHS and the evidentiatio of CIV as direct target of NaHS among mitochondrial respiration complexes are complemented and integrated by the NaHS inhibition of state 3 and state 4 respiration, whose ratio is unaffected by NaHS irrespective of CI or CII substrates. To sum up, NaHS reduces the electron flow in the OXPHOS system without affecting ATP synthesis (Fig 7).

Isolated adult cardiac myocytes exposed to 100 μM NaHS for 30 min showed a delayed cardioprotection [48]. Ischemia/reperfusion injury is known to be attenuated by blocking the formation and opening of the PTP [49]. Present data show that NaHS-treated swine heart mitochondria can avoid an uncontrolled Ca^{2+} release from mitochondria, associated with the collapse of the membrane potential (Fig. 7). Indeed, the CRC has a stepped course in the presence of NaHS, as well as RR trend, and does not show the typical profile where Ca^{2+} addition causes a sharp increase in fluorescence followed by a gradual decline as mitochondria take up Ca^{2+} (Fig. 7A). Finally, as repeated Ca^{2+} pulses trigger PTP opening, a large increase in fluorescence corresponds to the complete release of mitochondrial calcium. The PTP desensitization by NaHS seems to be related to the concomitant hindrance of mitochondrial Ca^{2+} uptake. In control mitochondria PTP opening is responsible for an abrupt IMM depolarization, as shown by the steep JC-10 fluorescence ratio increase upon Ca^{2+} addition (Fig. 7B). Conversely, in NaHS treated mitochondria the gradual increase of JC-10 ratio is probably due to the inhibition of mitochondrial respiration that reduces membrane potential. Moreover, the Ca^{2+} leak prior to Ca^{2+} pulse would suggest that control and NaHS-treated mitochondria differ in their conformation/structure. Most likely, the different structural properties are not necessarily related to mPTP opening, but to the inhibition of the mitochondrial Ca^{2+} uptake or, more generally, of Ca^{2+} cycle [39,50,51]. Consistently, the inhibition of mitochondrial respiration by NaHS may decrease the transmembrane protonmotive force, thus impairing the ion cycles which involve the Ca^{2+} uniport and the Ca^{2+} efflux by a Na^+ -

dependent pathway of $\text{Na}^+/\text{Ca}^{2+}$ antiport and a Na^+/H^+ antiport or Na^+ -independent pathway that has been suggested to occur via a $\text{Ca}^{2+}/\text{H}^+$ exchanger are all linked to the proton and calcium circuits [52].

Since H_2S can behave as the good, the bad and the ugly depending on the cell environment and the concentration, the present findings lead us to think that a negative effect on mitochondrial respiration may have at the same time the positive effect of preventing or delaying PTP opening.

5. Conclusion

The present work points out that all shown the sulfide effects on mitochondrial bioenergetics are not dependent on post-translational modifications of protein thiols that, even if chemically possible and well documented, under the conditions adopted are not operative in swine heart mitochondria. Most likely, the multiple H_2S action mechanisms are differently exerted according to the cell microenvironment and assay conditions.

The pharmacological interest of sulfide and of sulfide donors is strengthened, since micromolar concentrations are proven to delay PTP opening even if at the cost of a decreased mitochondrial respiration, which mirrors an inhibited electron transfer to CIV. So, further studies are required to deepen wanted and unwanted concentration-dependent effects of H_2S , which being gaseous at physiological temperatures necessarily requires H_2S donors, in the perspective of the use of these compounds in therapy.

Author contributions

C.A. investigation; F.T. validation; M.F. resources; F.T., V.V., A.P. writing - review & editing; S.N. conceptualization, writing - original draft, supervision; A.P. funding acquisition.

Role of the funding source

This work was financed by the University of Bologna, Italy (Almaidea senior grant to AP).

Declaration of Competing Interest

The authors declare that they have no competing interests in this work.

Acknowledgements

Danilo Matteuzzi and Roberto Giusti (Department of Veterinary Medical Sciences, University of Bologna) are gratefully acknowledged for kindly conferring swine hearts from a local abattoir to Biochemistry laboratories.

References

- [1] P. Mitchell, Keilin's respiratory chain concept and its chemiosmotic consequences, *Science*. 206 (1979) 1148–1159.
- [2] P. Mitchell, Coupling of phosphorylation to electron and hydrogen transfer by a chemi-osmotic type of mechanism, *Nature*. 191 (1961) 144–148.
- [3] D.G. Nicholls, S.J. Ferguson, 5 - Respiratory Chains, in: D.G. Nicholls, S.J. Ferguson (Eds.), *Bioenergetics (Fourth Edition)*, Academic Press, Boston, 2013: pp. 91–157. <https://doi.org/10.1016/B978-0-12-388425-1.00005-1>.
- [4] J.A. Enríquez, Supramolecular Organization of Respiratory Complexes, *Annual Review of Physiology*. 78 (2016) 533–561. <https://doi.org/10.1146/annurev-physiol-021115-105031>.
- [5] J. Gu, M. Wu, R. Guo, K. Yan, J. Lei, N. Gao, M. Yang, The architecture of the mammalian respirasome, *Nature*. 537 (2016) 639–643. <https://doi.org/10.1038/nature19359>.
- [6] J.A. Letts, K. Fiedorczuk, L.A. Sazanov, The architecture of respiratory supercomplexes, *Nature*. 537 (2016) 644–648. <https://doi.org/10.1038/nature19774>.
- [7] R. Guo, S. Zong, M. Wu, J. Gu, M. Yang, Architecture of Human Mitochondrial Respiratory Megacomplex I2III2IV2, *Cell*. 170 (2017) 1247–1257.e12. <https://doi.org/10.1016/j.cell.2017.07.050>.
- [8] K.M. Davies, T.B. Blum, W. Kühlbrandt, Conserved in situ arrangement of complex i and III2 in mitochondrial respiratory chain supercomplexes of mammals, yeast, and plants, *Proceedings of the National Academy of Sciences of the United States of America*. 115 (2018) 3024–3029. <https://doi.org/10.1073/pnas.1720702115>.
- [9] E. Maranzana, G. Barbero, A.I. Falasca, G. Lenaz, M.L. Genova, Mitochondrial respiratory supercomplex association limits production of reactive oxygen species from complex i, *Antioxidants and Redox Signaling*. 19 (2013) 1469–1480. <https://doi.org/10.1089/ars.2012.4845>.
- [10] J.A. Letts, K. Fiedorczuk, G. Degliesposti, M. Skehel, L.A. Sazanov, Structures of Respiratory Supercomplex I+III2 Reveal Functional and Conformational Crosstalk, *Mol. Cell*. 75 (2019) 1131–1146.e6. <https://doi.org/10.1016/j.molcel.2019.07.022>.
- [11] H. Guo, S.A. Bueler, J.L. Rubinstein, Atomic model for the dimeric FO region of mitochondrial ATP synthase, *Science*. 358 (2017) 936–940. <https://doi.org/10.1126/science.aao4815>.
- [12] P. Paumard, J. Vaillier, B. Coulary, J. Schaeffer, V. Soubannier, D.M. Mueller, D. Brèthes, J.-P. di Rago, J. Velours, The ATP synthase is involved in generating mitochondrial cristae morphology, *EMBO J*. 21 (2002) 221–230. <https://doi.org/10.1093/emboj/21.3.221>.
- [13] H. Itoh, A. Takahashi, K. Adachi, H. Noji, R. Yasuda, M. Yoshida, K. Kinoshita, Mechanically driven ATP synthesis by F1-ATPase, *Nature*. 427 (2004) 465–468. <https://doi.org/10.1038/nature02212>.
- [14] S. Nesci, A. Pagliarani, C. Algieri, F. Trombetti, Mitochondrial F-type ATP synthase: multiple enzyme functions revealed by the membrane-embedded FO structure, *Crit. Rev. Biochem. Mol. Biol*. 55 (2020) 309–321. <https://doi.org/10.1080/10409238.2020.1784084>.
- [15] W. Junge, H. Sielaff, S. Engelbrecht, Torque generation and elastic power transmission in the rotary F(O)F(1)-ATPase, *Nature*. 459 (2009) 364–370. <https://doi.org/10.1038/nature08145>.
- [16] M. Yoshida, E. Muneyuki, T. Hisabori, ATP synthase--a marvellous rotary engine of the cell, *Nat. Rev. Mol. Cell Biol*. 2 (2001) 669–677. <https://doi.org/10.1038/35089509>.
- [17] W. Junge, N. Nelson, ATP synthase, *Annu. Rev. Biochem*. 84 (2015) 631–657. <https://doi.org/10.1146/annurev-biochem-060614-034124>.
- [18] G. Pinke, L. Zhou, L.A. Sazanov, Cryo-EM structure of the entire mammalian F-type ATP synthase, *Nat. Struct. Mol. Biol*. (2020). <https://doi.org/10.1038/s41594-020-0503-8>.
- [19] S. Nesci, A. Pagliarani, Emerging Roles for the Mitochondrial ATP Synthase Supercomplexes, *Trends Biochem. Sci*. 44 (2019) 821–823. <https://doi.org/10.1016/j.tibs.2019.07.002>.
- [20] C. Algieri, F. Trombetti, A. Pagliarani, V. Ventrella, C. Bernardini, M. Fabbri, M. Forni, S. Nesci, Mitochondrial Ca²⁺-activated F1 FO -ATPase hydrolyzes ATP and promotes the permeability transition pore, *Ann. N. Y. Acad. Sci*. 1457 (2019) 142–157. <https://doi.org/10.1111/nyas.14218>.
- [21] S. Nesci, The mitochondrial permeability transition pore in cell death: A promising drug binding bioarchitecture, *Medicinal Research Reviews*. 40 (2020) 811–817. <https://doi.org/10.1002/med.21635>.

- [22] P. Bernardi, A. Rasola, M. Forte, G. Lippe, The Mitochondrial Permeability Transition Pore: Channel Formation by F-ATP Synthase, Integration in Signal Transduction, and Role in Pathophysiology, *Physiol. Rev.* 95 (2015) 1111–1155. <https://doi.org/10.1152/physrev.00001.2015>.
- [23] G.K. Kolluru, X. Shen, C.G. Kevil, A tale of two gases: NO and H₂S, foes or friends for life?, *Redox Biol.* 1 (2013) 313–318. <https://doi.org/10.1016/j.redox.2013.05.001>.
- [24] L. Li, P. Rose, P.K. Moore, Hydrogen sulfide and cell signaling, *Annu. Rev. Pharmacol. Toxicol.* 51 (2011) 169–187. <https://doi.org/10.1146/annurev-pharmtox-010510-100505>.
- [25] K. Módis, Y. Ju, A. Ahmad, A.A. Untereiner, Z. Altaany, L. Wu, C. Szabo, R. Wang, S-Sulphydration of ATP synthase by hydrogen sulfide stimulates mitochondrial bioenergetics, *Pharmacol. Res.* 113 (2016) 116–124. <https://doi.org/10.1016/j.phrs.2016.08.023>.
- [26] S. Nesci, F. Trombetti, V. Ventrella, A. Pagliarani, Post-translational modifications of the mitochondrial F₁FO-ATPase, *Biochim. Biophys. Acta.* 1861 (2017) 2902–2912. <https://doi.org/10.1016/j.bbagen.2017.08.007>.
- [27] C. Szabo, C. Ransy, K. Módis, M. Andriamihaja, B. Murghes, C. Coletta, G. Olah, K. Yanagi, F. Bouillaud, Regulation of mitochondrial bioenergetic function by hydrogen sulfide. Part I. Biochemical and physiological mechanisms, *Br. J. Pharmacol.* 171 (2014) 2099–2122. <https://doi.org/10.1111/bph.12369>.
- [28] S. Nesci, V. Ventrella, F. Trombetti, M. Pirini, A. Pagliarani, The mitochondrial F₁FO-ATPase desensitization to oligomycin by tributyltin is due to thiol oxidation, *Biochimie.* 97 (2014) 128–137. <https://doi.org/10.1016/j.biochi.2013.10.002>.
- [29] M.M. Bradford, A rapid and sensitive method for the quantitation of microgram quantities of protein utilizing the principle of protein-dye binding, *Anal. Biochem.* 72 (1976) 248–254. <https://doi.org/10.1006/abio.1976.9999>.
- [30] C. Algieri, F. Trombetti, A. Pagliarani, V. Ventrella, S. Nesci, Phenylglyoxal inhibition of the mitochondrial F₁FO-ATPase activated by Mg²⁺ or by Ca²⁺ provides clues on the mitochondrial permeability transition pore, *Arch. Biochem. Biophys.* 681 (2020) 108258. <https://doi.org/10.1016/j.abb.2020.108258>.
- [31] V. Ventrella, S. Nesci, F. Trombetti, P. Bandiera, M. Pirini, A.R. Borgatti, A. Pagliarani, Tributyltin inhibits the oligomycin-sensitive Mg-ATPase activity in *Mytilus galloprovincialis* digestive gland mitochondria, *Comp. Biochem. Physiol. C Toxicol. Pharmacol.* 153 (2011) 75–81. <https://doi.org/10.1016/j.cbpc.2010.08.007>.
- [32] S. Nesci, F. Trombetti, M. Pirini, V. Ventrella, A. Pagliarani, Mercury and protein thiols: Stimulation of mitochondrial F₁FO-ATPase and inhibition of respiration, *Chem. Biol. Interact.* 260 (2016) 42–49. <https://doi.org/10.1016/j.cbi.2016.10.018>.
- [33] B. Chance, G.R. Williams, Respiratory enzymes in oxidative phosphorylation. III. The steady state, *J Biol Chem.* 217 (1955) 409–427.
- [34] B. Chance, G.R. Williams, W.F. Holmes, J. Higgins, Respiratory enzymes in oxidative phosphorylation. V. A mechanism for oxidative phosphorylation, *J Biol Chem.* 217 (1955) 439–451.
- [35] R.W. Estabrook, [7] Mitochondrial respiratory control and the polarographic measurement of ADP : O ratios, in: *Methods in Enzymology*, Academic Press, 1967: pp. 41–47. [https://doi.org/10.1016/0076-6879\(67\)10010-4](https://doi.org/10.1016/0076-6879(67)10010-4).
- [36] O. Kabil, R. Banerjee, Redox biochemistry of hydrogen sulfide, *J Biol Chem.* 285 (2010) 21903–21907. <https://doi.org/10.1074/jbc.R110.128363>.
- [37] V. Vitvitsky, J.L. Miljkovic, T. Bostelaar, B. Adhikari, P.K. Yadav, A.K. Steiger, R. Torregrossa, M.D. Pluth, M. Whiteman, R. Banerjee, M.R. Filipovic, Cytochrome c Reduction by H₂S Potentiates Sulfide Signaling, *ACS Chem Biol.* 13 (2018) 2300–2307. <https://doi.org/10.1021/acscchembio.8b00463>.
- [38] S. Nesci, V. Ventrella, F. Trombetti, M. Pirini, A. Pagliarani, Tributyltin (TBT) and mitochondrial respiration in mussel digestive gland, *Toxicol In Vitro.* 25 (2011) 951–959. <https://doi.org/10.1016/j.tiv.2011.03.004>.
- [39] V. Algieri, C. Algieri, L. Maiuolo, A. De Nino, A. Pagliarani, M.A. Tallarida, F. Trombetti, S. Nesci, 1,5-Disubstituted-1,2,3-triazoles as inhibitors of the mitochondrial Ca²⁺-activated F₁FO-ATP(hydrol)ase and the permeability transition pore, *Ann N Y Acad Sci.* (2020). <https://doi.org/10.1111/nyas.14474>.

- [40] M. Bragadin, T. Pozzan, G.F. Azzone, Kinetics of Ca²⁺ carrier in rat liver mitochondria, *Biochemistry*. 18 (1979) 5972–5978.
- [41] K. Módis, E.M. Bos, E. Calzia, H. van Goor, C. Coletta, A. Papapetropoulos, M.R. Hellmich, P. Radermacher, F. Bouillaud, C. Szabo, Regulation of mitochondrial bioenergetic function by hydrogen sulfide. Part II. Pathophysiological and therapeutic aspects, *Br. J. Pharmacol.* 171 (2014) 2123–2146. <https://doi.org/10.1111/bph.12368>.
- [42] B.D. Paul, S.H. Snyder, K. Kashfi, Effects of hydrogen sulfide on mitochondrial function and cellular bioenergetics, *Redox Biol.* 38 (2020) 101772. <https://doi.org/10.1016/j.redox.2020.101772>.
- [43] A.K. Mustafa, M.M. Gadalla, N. Sen, S. Kim, W. Mu, S.K. Gazi, R.K. Barrow, G. Yang, R. Wang, S.H. Snyder, HS signals through protein S-Sulfhydration, *Science Signaling*. 2 (2009). <https://doi.org/10.1126/scisignal.2000464>.
- [44] P. Nicholls, J.K. Kim, Sulphide as an inhibitor and electron donor for the cytochrome c oxidase system, *Can J Biochem.* 60 (1982) 613–623. <https://doi.org/10.1139/o82-076>.
- [45] M. Gubern, M. Andriamihaja, T. Nübel, F. Blachier, F. Bouillaud, Sulfide, the first inorganic substrate for human cells, *FASEB Journal*. 21 (2007) 1699–1706. <https://doi.org/10.1096/fj.06-7407com>.
- [46] M.A. Powell, G.N. Somero, Hydrogen sulfide oxidation is coupled to oxidative phosphorylation in mitochondria of *Solemya reidi*, *Science*. 233 (1986) 563–566. <https://doi.org/10.1126/science.233.4763.563>.
- [47] J.G. Fedor, J. Hirst, Mitochondrial Supercomplexes Do Not Enhance Catalysis by Quinone Channeling, *Cell Metabolism*. 28 (2018) 525–531.e4. <https://doi.org/10.1016/j.cmet.2018.05.024>.
- [48] J.W. Calvert, W.A. Coetzee, D.J. Lefer, Novel insights into hydrogen sulfide--mediated cytoprotection, *Antioxid Redox Signal*. 12 (2010) 1203–1217. <https://doi.org/10.1089/ars.2009.2882>.
- [49] G. Morciano, C. Giorgi, M. Bonora, S. Punzetti, R. Pavasini, M.R. Wieckowski, G. Campo, P. Pinton, Molecular identity of the mitochondrial permeability transition pore and its role in ischemia-reperfusion injury, *J. Mol. Cell. Cardiol.* 78 (2015) 142–153. <https://doi.org/10.1016/j.yjmcc.2014.08.015>.
- [50] S. Marchi, V.A.M. Vitto, S. Patergnani, P. Pinton, High mitochondrial Ca²⁺ content increases cancer cell proliferation upon inhibition of mitochondrial permeability transition pore (mPTP), *Cell Cycle*. 18 (2019) 914–916. <https://doi.org/10.1080/15384101.2019.1598729>.
- [51] D.G. Nicholls, S.J. Ferguson, 9 - Cellular Bioenergetics, in: D.G. Nicholls, S.J. Ferguson (Eds.), *Bioenergetics (Fourth Edition)*, Academic Press, Boston, 2013: pp. 255–302. <https://doi.org/10.1016/B978-0-12-388425-1.00009-9>.
- [52] E. Murphy, C. Steenbergen, Regulation of Mitochondrial Ca²⁺ Uptake, *Annu Rev Physiol.* (2020). <https://doi.org/10.1146/annurev-physiol-031920-092419>.

Figure

Figure 1. Response of the mitochondrial Mg^{2+} and Ca^{2+} -dependent F_1F_0 -ATPase activities to increasing NaHS concentrations. Data, expressed as percentage of the Mg^{2+} -dependent F_1F_0 -ATPase (A) and Ca^{2+} -dependent F_1F_0 -ATPase (B) in absence of NaHS, represent the mean \pm SD from three independent experiments carried out on different mitochondrial preparations. * indicates significant differences with respect to the control ($P \leq 0.05$).

Figure 2. Mg^{2+} and Ca^{2+} -dependent F_1F_0 -ATPase activities of NaHS treated mitochondria in the presence of thiol-reagents. The effect of 50 μM DTE (A and B) or 1 mM GSSG were evaluated in the absence (green) (■) and in the presence of 100 μM NaHS (red) (■). Data, expressed as percentage of the Mg^{2+} -dependent F_1F_0 -ATPase and Ca^{2+} -dependent F_1F_0 -ATPase in absence of NaHS, represent the mean \pm SD from three independent experiments carried out on different pools. Different letters indicate significantly different values within each treatment ($P \leq 0.05$).

Figure 3. NaHS effects on mitochondrial respiration. NADH- O_2 oxidoreductase activity (A) and Succinate- O_2 oxidoreductase activity (B) in the presence of increasing NaHS concentrations. All points represent the mean \pm SD from three independent experiments carried out on different mitochondrial preparations.

Figure 4. Evaluation of the putative sulfhydrylation involvement in the inhibition of the mitochondrial respiration by NaHS. The NADH- O_2 oxidoreductase activity (A,B) and the Succinate- O_2 oxidoreductase activity (C,D) were assayed in the absence (green) (■) or in presence of 50 μM DTE (red) (■). 100 μM NaHS was added to reaction system containing mitochondrial suspensions energized with either 75 μM NADH or 10 mM succinate as substrates. The NaHS solution was added sequentially before or after DTE. Data represent the mean \pm SD of three different experiments. Different letters indicate significantly different values ($P \leq 0.05$).

Figure 5. Response of the cytochrome *c* oxidase activity to NaHS. The enzyme activity was spectrophotometrically assayed in the presence of 10 μM reduced cytochrome *c* as substrate at different NaHS concentrations. Data represent the mean \pm SD (vertical bars) from three independent experiments carried out on different mitochondrial preparations.

Figure 6. Threshold plots of mitochondrial respiration. Each point represents the NADH- O_2 oxidoreductase (A) and the succinate- O_2 oxidoreductase (B) percentage of residual activity as a function of percent inhibition of cytochrome *c* oxidase by the NaHS concentrations shown at the right side of the plot. All points represent the mean \pm SD (horizontal bars) from three independent experiments carried out on different mitochondrial preparations.

Figure 7. NaHS effects on selected oxidative phosphorylation parameters: state 3 and 4 respiration and their ratio. Glutamate/malate- (A) and Succinate- (B) stimulated mitochondrial respiration in the presence (red) (■) and in the absence (green) (■) of 30 μM NaHS. All bars represent the mean \pm SD from three independent experiments carried out on different mitochondrial preparations. * indicates significantly different values ($P \leq 0.05$).

Figure 8. Evaluation of PTP opening in intact mitochondrial preparations. Representative curves (A) of the calcium retention capacity (CRC) detected as Fura-FF ratio and (B) and the membrane potential ($\Delta\phi$) detected as JC-10 ratio. CRC and $\Delta\phi$ were monitored in response to subsequent 10 μ M CaCl_2 pulses (shown by the triangles), as detailed in the 2.5 section. The NaHS concentrations were selected on the basis of IC_{50} values obtained on mitochondrial respiration and on the Ca^{2+} -activated F_1F_0 -ATPase. RR, Ruthenium Red. Three independent experiments were carried out on three different mitochondrial preparations.

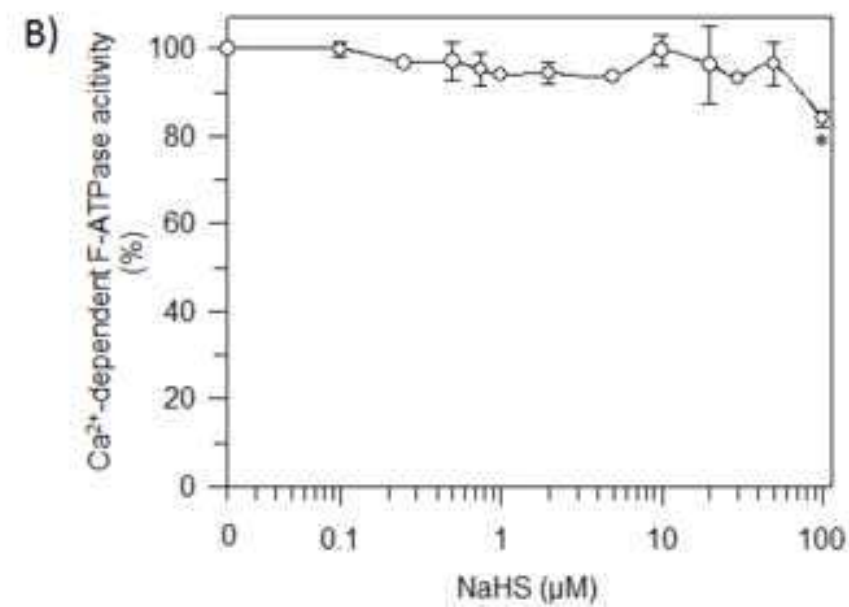
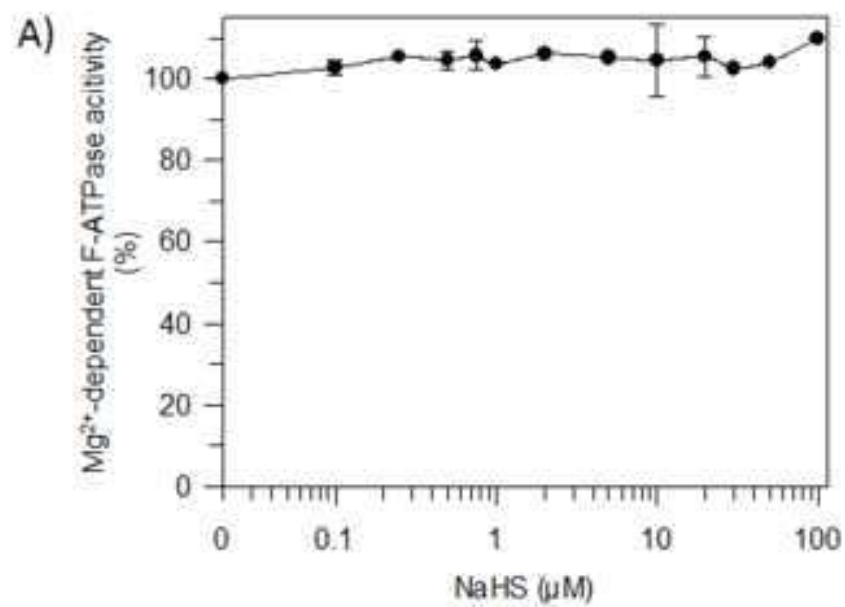


Figure 2

[Click here to access/download;Figure;Figure 2.tif](#)

